HHS Public Access

Author manuscript

Nat Chem Biol. Author manuscript; available in PMC 2010 September 01.

Published in final edited form as:

Nat Chem Biol. 2010 March ; 6(3): 218–224. doi:10.1038/nchembio.312.

The 2′-OH group at the group II intron terminus acts as a proton shuttle

Michael Roitzsch[1,2,3], **Olga Fedorova**[1,2], and **Anna Marie Pyle**[1,2,*]

[1] Howard Hughes Medical Institute, Yale University, New Haven, CT 06520, USA

[2] Department of Molecular Biophysics and Biochemistry, Yale University, New Haven, CT 06520, USA

[3] Fakultät Chemie, Technische Universität Dortmund, 44221 Dortmund, Germany

Abstract

Group II introns are self-splicing ribozymes that excise themselves from precursor RNAs and catalyze the joining of flanking exons. Excised introns can behave as parasitic RNA molecules, catalyzing their own insertion into DNA and RNA via a reverse-splicing reaction. Previous studies have identified mechanistic roles for various functional groups located in the catalytic core of the intron and within target molecules. Here we introduce a new method for synthesizing long RNA molecules with a modified nucleotide at the 3′-terminus. This modification allows us to examine the mechanistic role of functional groups adjacent to the reaction nucleophile. During reverse-splicing, the 3′-OH group of the intron terminus attacks the phosphodiester linkage of spliced exon sequences. Here we show that the adjacent 2′-OH group on the intron terminus plays an essential role in activating the nucleophile by stripping away a proton from the 3′-OH and then shuttling it from the active-site.

Group II introns are a class of large ribozymes that catalyze both their own excision from precursor RNAs and their subsequent insertion into new genomic targets (intron mobility)1. They are found within the organellar genes of higher plants and fungi as well as in many bacteria, proteobacteria, blue algae and some animals2. The dispersal and evolution of group II introns has had a profound influence on the organization and regulation of most terrestrial genomes3. Group II introns share a characteristic secondary structure consisting of six functional domains (Figure 1a)3 and their tertiary structural features have been revealed through extensive biochemical and crystallographic analysis4–7.

---

*To whom correspondence should be addressed. anna.pyle@yale.edu.

Author contributions

M.R. designed and performed kinetic experiments and analyzed the data. M.R. designed and conducted the method for generation of 3′-terminally modified RNAs including their purity control, but with exception of experiments involving fluorescein labeling. O.F. designed and performed all control experiments involving fluorescein labeling and prepared the modified DNA primers and all synthetic RNA oligonucleotides. M.R. interpreted the results and wrote the manuscript. O.F. helped interpreting the results. O.F. and A.M.P. edited the manuscript. A.M.P provided funding for the research and supervised all experimentation.

The authors declare no competing financial interests.

Group II introns catalyze excision from precursor RNAs through a two step self-splicing reaction (Figure 1b). Depending on the nucleophile in the first splicing step, the intron is excised in a lariat form with a 2′,3′,5′-branched adenosine, or in a linear form with a 5′-terminal phosphate8–9. The second splicing step is always a transesterification, in which the terminal 3′-OH group of the 5′-exon attacks the phosphate at the 3′-splice site. This step is highly reversible and it is typically quite rapid10–11. Unlike the well-studied first step of splicing, the second step is the most poorly understood stage of the splicing pathway.

Second-step reversal (reverse-splicing) is of great mechanistic interest because excised group II introns can behave as retroelements, integrating themselves into new genomic locations through a complex series of events that involve direct insertion into the DNA1. This process is initiated by a reverse-splicing reaction, in which free intron binds and inserts itself into target sequences that resemble the original flanking exons. Although the entire transposition process requires many steps and additional protein cofactors, it begins with the catalysis of reverse-splicing12. A clear mechanistic understanding of this basic reaction is therefore central to our knowledge of group II intron mobility and to the application of group II introns as tools for genomic manipulation and biotechnology.

Reverse-splicing into single stranded RNA does not require protein cofactors and it is particularly efficient with linear intron molecules11. Linear introns only catalyze the first step of reverse-splicing, which is advantageous because it facilitates the design of simple kinetic experiments and a straightforward kinetic framework (Figure 1c). Through a series of enzymological experiments on the mechanism and pH dependence of reverse-splicing, we have shown previously that the chemical reaction is rate limiting for the first step of reverse-splicing11. Reverse-splicing therefore provides a way to monitor chemical catalysis by group II introns and to understand the functional groups that contribute to stabilization of the transition-state.

A number of studies have elucidated mechanistic features of self-splicing, resulting in a basic model for chemical catalysis (Figure 1d)13. Functional group substitutions have provided particularly useful probes of specific atoms that are involved in the chemical mechanism. For example, kinetic analysis of intron constructs containing chiral phosphorothioate substitutions at the splice sites reveals the stereoisomeric preference of reaction14–16. These experiments also reveal that both steps of splicing proceed with inversion of configuration at the scissile phosphate, consistent with nucleophilic substitution reactions that proceed through an S_N2 mechanism14. Similarly, 3′-thiolate substitution and metal ion rescue experiments in the presence of metal ions with stronger ligand affinity such as Mn^{2+} reveal sites of catalytic metal ion coordination on the substrate17. Based on these results, at least two Mg^{2+} ions were proposed to participate in the catalysis of phosphodiester cleavage18,19. Indeed, a recent crystal structure of the intron confirms that the active site contains two Mg^{2+} ions separated by a distance of 3.9 Å, which is typical of enzymes that cleave via a two-metal ion mechanism6.

Despite the importance of metal ions for chemical reactivity by group II introns, there are many other functional groups that may contribute to the chemical mechanism. An example is the 2′-OH group at the cleavage site of RNA target oligonucleotides, which are

hydrolytically cleaved by truncated ribozyme constructs of the intron20. Substitution of the cleavage site 2′-OH group with 2′-H results in a 16-fold decrease in the chemical rate constant20. A more comprehensive study, in which a large number of 2′-modifications were tested comes to the conclusion that the 2′-OH mediates interactions with solvent water molecules21.

In this study, we set out to determine the precise mechanistic role of the 2′-OH group on the intron terminus, adjacent to the 3′-OH group that acts as the nucleophile during reverse-splicing. The role of the terminal 2′-OH group has never been examined in the context of reverse-splicing, despite the fact that it is located in an ideal position to influence intron reactivity. By substituting this 2′-OH group with diverse functional groups and measuring the resultant effects on the rate-constant for transesterification, we have determined that this group is essential for the reactivity of free group II intron molecules. In addition, detailed chemogenetic studies show that this 2′-OH group plays a key role in deprotonating the nucleophile and shuttling the proton away from the cleavage site.

RESULTS

Experimental design

As a first step in this study, we designed a new synthetic route to intron molecules that contain modified functional groups, such as 2′-H, 2′-F, 2′-OMe and 2′-NH_2 substitutions, on the 3′-terminal nucleotide. Using the ai5γ intron from *S. cerevisiae*, we generated an intron construct in which domain 4 was shortened to a hairpin. This modification reduces the intron size without altering the catalytic properties. The approach for introduction of modified nucleotides is similar to 3′-end labeling using the Klenow fragment22: Intron molecules that lack the terminal nucleotide (a uridine) were transcribed from a corresponding template DNA, resulting in a shortened transcript that is referred to as “ai5γ-1”. Normally, transcription by the T7 RNA polymerase results in a ragged 3′-end, in which additional nucleotides (+1, +2 and more) are added by the enzyme23. As in our previous work11, precisely terminated transcription products were created by using special PCR-generated DNA templates, which contain a 2′-OMe modification at the penultimate nucleotide of the template strand. This modification suppresses incorporation of untemplated nucleotides24. A short DNA oligonucleotide was then hybridized to the 3′-terminus of the intron, resulting in a single overhanging 5′-deoxyadenosine (Figure 2a), which permitted the incorporation of a single uridine at the end of the intron RNA by the Klenow fragment.

While intron molecules bearing a 2′-H at the terminus can be easily synthesized using this method, the Klenow fragment has DNA polymerase specificity, making it difficult to incorporate ribonucleotides or modified nucleotides25. This discrimination between ribo- and deoxynucleotides is achieved by a glutamic acid residue(position 710) that sterically blocks the 2′-OH group of ribonucleotides. To circumvent this problem, we utilized the E710A mutant of the Klenow fragment in order to generate diverse, terminally modified RNAs. This alanine mutant incorporates ribonucleotides more efficiently than the wild-type enzyme25, however we found that the reaction requires added Mn^{2+} to facilitate efficient extension with various 2′-modified nucleotide analogs.

In order to monitor extension products of the mutant Klenow fragment, we cleaved each modified intron RNA with a DNAzyme near the 3′-end of the intron26. The resulting fragments were then 5′-end labeled using ^{32}P and visualized by gel electrophoresis (Figure 2b). The mobility of each fragment indicates that the corresponding modified nucleotide was successfully incorporated. None of the samples contained residual unextended ai5γ-1 transcripts or products that were extended by more than one nucleotide. As a control, we generated wild-type intron by extension of ai5γ-1 transcripts with rUTP using the same protocol. Reactivity of this RNA was identical to that of full-length wild-type intron (Figure 2c), indicating that the extension procedure has no adverse effects.

To further validate the assay and to demonstrate complete incorporation of the 2′-NH_2 substituent at the 3′-terminus (which is a particularly important variant for this study, *vide infra*), we 5′-^{32}P-end-labeled the 3′-terminal 2′-OH and 2′-NH_2 samples and then incubated them with fluorescein isothiocyanate. The reaction products were then visualized by radioanalytic and fluorescent imaging, which revealed that only the 2′-amino terminal intron was labeled with dye (Supplementary Figure 1a). In addition, the reaction products were cut into shorter fragments with a DNAzyme, 5′-^{32}P labeled and then subjected to PAGE, which revealed that the 2′-NH_2-modified variant was quantitatively labeled with fluorescein, as it displays a complete gel-shift after dye labeling (Supplementary Figure 1b) (see Methods). These results demonstrate that the 2′-NH_2 extension product is pure and that it unequivocally contains a terminal amine.

Development of the reverse-splicing assay for modified introns

The role of the 3′-terminal 2′-OH group was studied using a reverse-splicing assay in which the chemical step of transesterification is rate-limiting11. Each modified intron RNA was incubated with a 3′-end labeled RNA oligonucleotide substrate (24 nts) that corresponds to the sequence of the ai5γ spliced exon product (Figure 3a,b). Effects caused by substrate binding and release were minimized by using single turnover conditions, i.e., reacting trace amounts of labeled substrate with excess linear intron (Figure 3c–g). Fractions of precursor and evolving products were fit to the kinetic framework shown in Figure 1c using kinetic simulations27.

The intron catalyzes two reactions: reverse-splicing, which covalently attaches the 3′-exon section of the substrate to the intron, and spliced exon reopening (SER), which is the irreversible hydrolytic cleavage of the substrate at the splice site junction. The SER reaction provides a useful internal control, because its efficiency is independent of modifications at the intron terminus, thereby providing an independent metric for the proper folding and active-site integrity of the modified introns.

The ai5γ-1 transcript provides another useful control in these experiments (Figure 3c). Since this intron RNA lacks the 3′-terminal uridine, it cannot perform reverse-splicing. However, it catalyzes SER, indicating that it folds correctly into a catalytically active form. Overexposed gels show trace amounts (<0.3%) of reverse-splicing product, which evolves with rate contants that are typical for the wild type intron, indicating that trace amounts of wild-type molecules are present. Since ai5γ-1 is the precursor for all modified RNAs, this

impurity was present in the same amount in all samples, allowing a simple correction of the experimental data.

Reactivity of the terminally modified introns

The various 3′-terminally modified intron RNAs displayed differing levels of activity (Figure 3d–g). The 2′-deoxynucleotide modification resulted in complete loss of reverse-splicing product (Figure 3d), which conclusively demonstrates that the terminal 2′-OH group plays an essential mechanistic role during reverse-splicing. Based on this finding, at least four potential roles for the 2′-OH are possible: (I) The 3′-*endo* sugar conformation, which is preferred by ribonucleotides but not by deoxynucleotides, may be required for catalysis. (II) The deprotonation of the 3′-OH group could be supported by an inductive effect of the 2′-OH group. (III) The 2′-OH group could accept a proton from the 3′-OH group during nucleophilic attack on the splice site phosphate. (IV) The 2′-OH group may contribute to catalysis by binding of a critical metal ion. By examining the behavior of the remaining 2′-modified derivatives, it was possible to differentiate between these possible models.

The 2′-fluorouridine derivative has a preference for the 3′-*endo* sugar conformation and 2′-F substituents have an even stronger inductive effect than a 2′-OH group. Thus, the 2′-F substitution allows us to test whether these two characteristics stimulate reverse-splicing. The 2′-fluorouridine modification resulted in a complete loss of reverse-splicing activity (Figure 3e), suggesting that neither the electron withdrawing effect nor the preference for the 3′-*endo* sugar conformation is the predominant function of this group. Although the 2′-F substituent has three lone electron pairs, it is a poor hydrogen bond acceptor and is therefore unlikely to accept a proton from the 3′-OH group28.

By contrast, 2′-amino groups have one lone electron pair and they are good hydrogen bond acceptors. In the reverse-splicing assay, the terminally 2′-NH_2 modified intron readily underwent reverse-splicing(Figure 3f). At pH 7.8, reverse-splicing was only 3 times slower compared to wild-type intron. However, the 2′-NH_2 modified intron showed pronounced pH dependence with dramatically decreased activity under acidic conditions: at pH 4.8, reverse-splicing is 100-fold slower compared to wild-type intron under the same conditions. In order to evaluate this effect more carefully, we determined the rate constant for reverse-splicing at various pH values. The logarithm of the rate constants was plotted against the pH value, revealing a linear correlation with a slope of 2 in the acidic pH range (Supplementary Figure 2). For comparison, the wild-type intron shows a slope of 1 in an analogous plot11. The experimental data can be described by equation 1, which was derived for a system in which two distinct acidic sites must be deprotonated to permit the reaction. The observed rate constant k_{obs} approaches the maximum rate k_{max} when the pH exceeds both pK_a values.

$$\log k_{obs} = \log\left(k_{max} \cdot \frac{10^{-pK_{a,1}}}{10^{-pK_{a,1}} + 10^{-pH}} \cdot \frac{10^{-pK_{a,2}}}{10^{-pK_{a,2}} + 10^{-pH}}\right) \quad [1]$$

The pK_a value of the more acidic site was 6.1, which matched the pK_a expected for the 2′-NH_3^+ group29. These data indicate that only the 2′-NH_2, but not the 2′-NH_3^+ moiety

supports reverse-splicing, and thus that the free lone electron pair is required. This suggests that the 2′-substituent may act as a proton acceptor, helping to deprotonate the 3′-OH group.

However, the results are also consistent with catalytic metal ion binding by the terminal 2′-group. To test the latter model, we performed experiments in the presence of Mn^{2+}. Amino groups prefer binding to Mn^{2+} over Mg^{2+} by ≈20-fold30. Thus, Mn^{2+} should significantly stimulate reverse-splicing of the 2′-NH_2 modified intron if the 2′-group coordinates a metal ion. However, addition of 10 mM Mn^{2+} at pH 7.8 resulted in a negligible 1.2 fold increase in the rate constant for reverse-splicing, which is inconsistent with a mechanistic role involving metal ion binding.

Thus far, the data are consistent with a mechanism in which the 2′-OH group accepts the proton from the 3′-OH group, which raises the question of the subsequent fate of this proton. An obvious model is that the 2′-OH_2^+ intermediate donates the other proton quickly to a basic group located outside the reaction site. This model can be tested with the 2′-OMe modified intron (Figure 3g). The 2′-OMe group can accept a proton like the 2′-OH group, but it cannot pass the positive charge out of the active site by donating it to an external acceptor. The experimental results indicate that the 2′-OMe modified intron can catalyze reverse-splicing, but it is highly inefficient: only a small fraction (3%) of reverse-splicing product was formed and the rate constant was approximately 25 times slower than that of wild type intron (rates obtained at pH 6.3). Hence, experiments with this modified intron are consistent with an additional proton transport function for the terminal 2′-OH group.

DISCUSSION

In this work, we incorporated modified nucleotides at the 3′-terminus of a group II intron, adjacent to the reaction nucleophile for reverse-splicing. We then monitored the effect of these substitutions on the chemical rate constants and pH sensitivity of the reaction. Based on the results of these experiments, we derived a mechanism for stabilization of the transition-state during reverse-splicing, which is the crucial first step during mobility and transposition by group II introns. This mechanism, which has parallels with reactivity of both protein and RNA enzymes, has implications for the mechanism of forward-splicing by group II introns and the spliceosome.

The study was contingent on the development of a new approach for incorporating modified nucleotides at the 3′-terminus of transcribed intron RNA molecules (Figure 2). The procedure first involved the transcription of an intron RNA with a precisely defined terminus that is one nucleotide shorter than the desired product. The resultant transcript was then extended by one nucleotide with various 2′-substituted NTP-analogs using the E710A mutant of the Klenow fragment in the presence of Mn^{2+}. While used here to add a single nucleotide, the method could be adapted to add more than one nucleotide to appropriately shortened transcripts in order to generate RNAs with diverse, and potentially multiple substituents near the 3′-end. In addition, RNAs with modifications of any identity, at almost any position, could then be added by enzymatic ligation of synthetic RNAs to the modified transcript. Thus the approach provides a convenient and efficient route to homogeneous modified RNAs of high quality that are otherwise difficult to synthesize or which contain

multiple modified groups. Given the large number of commercially available modified NTPs, this approach considerably expands the repertoire of modifications and tags that can be incorporated into RNA transcripts.

Reverse-splicing catalyzed by the 3′-terminally modified introns was kinetically investigated. The lack of reactivity by introns containing terminal 2′-H and 2′-F substituents indicates that the 2′-hydroxyl group at the terminus of free introns plays a critical role in stimulating reactivity of the adjacent 3′-hydroxyl group, which is the nucleophile during reverse-splicing(Figure 3d,e). Insights into the probable role of the 2′-OH group were provided by introns containing a terminal 2′-NH_2 group, which catalyzed reverse-splicing at high pH almost as efficiently as the wild-type intron (Figure 3f). Importantly, the 2′-NH_2 group becomes protonated at low pH (pK = 6.1), resulting in a dramatic deceleration in reverse-splicing activity (Supplementary Figure 2). This suggests that the lone electron pair on 2′-NH_2 or 2′-OH plays a direct and key role in chemical catalysis by intron molecules. Taken together, the results suggest a specific chemical mechanism for reverse-splicing(Figure 4). The reaction is initiated by nucleophilic attack of the 3′-oxygen, which must first be deprotonated. We propose that the 2′-OH group accepts the proton from the 3′-oxygenandforms an intermediate involving a positively charged 2′-OH_2^+ group. This intermediate is stabilized by a hydrogen bonding network through which the extra proton (and charge) is passed to an external general base, thereby driving the reaction forward. The same transport pathway can be used by the 2′-NH_2 modified intron, explaining the enhanced efficiency at high pH. The external base is likely to be some other functional group within the intron active site, such as a metal-coordinated water molecule, or a nucleobase with a perturbed pK_a value31. That the 2′-OH not only accepts a proton, but must also pass it along, is suggested by experiments with the 2′-OMe modified intron (Figure 3g). Protonation of a 2′-OMe group is only slightly more difficult than protonation of 2′-OH(the pK_a values are similar32). Thus, the 2′-OMe group would be expected to readily accept a proton, and to form a 2′-$OHMe^+$ intermediate. However, due to geometrical constraints, a 2′-$OHMe^+$ cannot readily pass the charge into a hydrogen bonding network. An additional rotation of the 2′-$OHMe^+$ group would be required to release the proton to an external acceptor, increasing the probability that the proton is simply returned to the 3′-oxygen. Consistent with this notion, the 2′-OMe modified intron displays slow reverse-splicing activity with low product amplitude, suggesting facile reversibility. In contrast to the terminal 2′-NH_2 and 2′-OMe substitutions, the 2′-F substitution prevents reverse-splicing completely (Figure 3e). This observation agrees well with the proposed model: despite its three lone electron pairs, carbon-bound fluorine is a poor hydrogen bond acceptor28.

The 2′-OH group does not appear to be a metal binding site. It is known that several oxygen atoms in the catalytic core coordinate catalytically important metal ions15,33. These contacts stabilize developing charges in the transition-state or are necessary for arranging the metal ions properly in the catalytic center5–6,15,17–18. In view of this, the 2′-OH group of the terminal group II intron nucleotide might likewise be expected to coordinate catalytically important metal ions. As proposed for group I introns34, it could coordinate the same metal ion as the neighboring 3′-OH group to further stabilize and orient it. Alternatively, the 2′-OH group could bind a third metal ion, which would withdraw electron

density from the sugar ring, facilitating deprotonation of the 3′-OH group. In both of these cases, however, the 2′-OH group would be playing a supporting, rather than critical role during catalysis. Removal of the 2′-OH group would be expected to reduce rates, but not obliterate reverse-splicing altogether, which contradicts our observations. Additional experimental data that rule out a key role for metal coordination come from experiments with the 2′-NH_2 modified intron. The amino group has a pronounced preference for Mn^{2+} over Mg^{2+}30, and supplementation of the reaction with Mn^{2+} is expected to significantly increase the reverse-splicing activity of a modified intron in which the terminal 2′-NH_2 directly coordinates a metal ion. However, the addition of 10 mM Mn^{2+} did not significantly increase reverse-splicing activity. Thus, it is unlikely that a major role for the terminal 2′-OH involves the coordination of catalytic metal ions. There is no doubt that metal ions play a crucial role in group II intron catalysis, but other functional groups may likewise play an essential role. An abundance of evidence from studies of other ribozymes (particularly the smaller hairpin and hepatitis delta ribozymes) indicates that nucleobases and other RNA functional groups can play direct roles in the chemical mechanism of catalysis by RNA. Given the complexity of the group II intron active-site structure, and the abundance of conserved nucleotides at the catalytic core, it would be surprising if nucleotide functional groups failed to play a role in the mechanism.

Proton shuttling, as proposed in the present mechanism, appears to be a common mechanistic feature in ribozymes. The first ribozyme proposed to use a proton transfer mechanism was the Hepatitis Delta Virus (HDV) ribozyme. Self-cleavage by this ribozyme results in formation of a cyclic 2′,3′-phosphate at the intron terminus and a free 5′-OH group on the released fragment. In this reaction, a cytosine residue with an elevated pK_a (C75) donates a proton to the 5′-O leaving group and participates in an extended hydrogen bonding network35–36. A proton shuttling mechanism involving 2′-OH groups has been proposed for the *Tetrahymena* group I intron34. During the first splicing step, a hydrogen bonding network is believed to facilitate protonation of the 3′-oxygen leaving group. In that case, the network is proposed to extend from the vicinal 2′-OH group (which donates a proton) through a series of additional nucleotides, eventually transporting a proton from outside the core to the 3-oxygen leaving group34. Another study suggests that the 2′-OH group at the 3′-splice site of a group II intron donates a proton to stabilize the 3′-leaving group in that system37. Similarly, a proton shuttle involving 2′-OH groups appears to be crucial for peptide bond formation catalyzed by the ribosome38–39.

Our results have important implications for the mechanism of splicing by group II introns and the spliceosome. Given the principle of microscopic reversibility, a 2′-OH group that acts as a proton acceptor in the first stages of reverse-splicing will act as a proton donor during the second step of splicing. In the latter case, the 3′-hydroxyl on the terminal intron nucleotide is the leaving group; it experiences a build-up of negative charge during the transition-state, and it requires protonation for efficient release. The results provided here suggest that the vicinal 2′-OH supports this process and that proton donation from this group is likely to be assisted by a general acid moiety elsewhere in the intron. Perhaps most intriguing is that a similar system is likely to be at work during pre-mRNA processing by the eukaryotic spliceosome. While pre-mRNA introns do not reverse-splice (they are not

autocatalytic), it is becoming increasingly clear that the active-sites of group II introns and the spliceosome share many structural similarities5. In addition, splicing by group II introns and by the spliceosome share mechanistic parallels, as shown by comparative enzymological studies of functional group sensitivity in the two systems17,40. Thus, it is likely that the terminal 2′-OHgroup of pre-mRNA introns donates a proton to the 3′-OHleaving group as it is liberated during the second step of splicing. If this is true, then by extension, it is likely that the spliceosome contains a mechanistically essential general acid that limits the rate constant for the second step of splicing. This general acid group could be provided by a nucleobase within the U6 snRNA, a metal-coordinated water molecule, or a side-chain on the proximal Prp8 protein. As in previous mechanistic studies, insights from group II intron reactivity are likely to inform biochemical investigations into spliceosomal function and catalysis.

METHODS

Preparation of oligonucleotides

RNA substrate (5′-CGUGGUGGGACAUUUUC/ACUAUGU-3′) and the 2′-OMe modified primer ASai5γ-1 (5′-T**C**CCGATAGGTAGACCTTTACAAGTTTTCC-3′) were synthesized and deprotected as described41. Primer SB (5′-GAATTCTAATACGACTCACTATAGAGCGGTCTGAAAG-3′), ai5γ-1_splint (5′-TTATCCCGATAGGTAGACCTTTACAAG-3′), DNAzyme 1 (5′-TCCCGATAGGGGCTAGCTACAACGAAGACCTTTACAAG-3′), DNAzyme 2 (5′-AGACCTTTACAAGGGCTAGCTACAACGATTTCCCCC-3′) and DNAzyme 3 (5′-ATAGGTAGACCTTTAGGCTAGCTACAACGAAAGTTTTCCCC) were purchased from Invitrogen. The RNA substrate was 3′-end labeled with [^{32}P]pCp and T4 RNA ligase as described42.

Preparation of RNAs with substitutions at the 3′-terminus

The ai5γ-1 intron was transcribed with T7 RNA polymerase and PAGE purified. The template DNA was generated by PCR using sense primer SB and antisense primer ASai5γ-1. The antisense primer had a 2′-OMe modification at the penultimate nucleotide to suppress incorporation of untemplated nucleotides at the 3′-terminus of the transcripts24.

The ai5γ-1 transcripts were extended with either uridine-5′-triphosphate, 2′-deoxythymidine-5′-triphosphate, 2′-fluoro-2′-deoxyuridine-5′-triphosphate, 2′-amino-2′-deoxyuridine-5′-triphosphate or 2′-methoxy-2′-deoxyuridine-5′-triphosphate (Trilink Biotech). Extension was performed using the E710A mutant of the Klenow fragment43. A 500 μL volume of a mixture of 1 μM ai5γ-1, 6 μM ai5γ-1_splint, 20 mM Tris-HCl pH 7.5, 1 mM EDTA and 80 mM NaCl was heated for 2 min to 95°C and then cooled within 10 min to 42°C. Then 500 uL of a mixture of 2 mM DTT, 20 mM $MgCl_2$, 6mM $MnCl_2$, 200 μM of the respective nucleoside-5′-triphosphate and 5 μM of the E710A mutant Klenow fragment was added. The mixture was incubated for 90 minutes at 37°C. The extended intron RNA was PAGE purified.

Analysis of the terminally modified intron RNAs

The sequence, identity and length of the modified intron RNAs were examined by cleaving the downstream termini of Klenow-extended intron using site-directed DNAzymes26, and then evaluating the mobility of resultant fragments. DNAzyme 1 and DNAzyme 2 were designed to cleave 11 and 25 nucleotides upstream of the 3′-end of the extended intron RNA, respectively26. Both DNAzymes were 5′-phosphorylated with PNK (NEB) according to the manufacturers protocol to prevent 5′-labeling of remaining fragments during subsequent steps of the protocol.

A mixture of 0.2 μM extended intron, 15 μM DNAzyme 1 or DNAzyme 2, 10 mM Tris-HCl pH 7.5 and 1 mM EDTA (8 μL total volume) was heated to 95 °C for 1 min and then cooled on ice for 1 min. Subsequently, 2 uL of a solution containing 300 mM $MgCl_2$ and 750 mM NaCl was added and the mixture was incubated at 37 °C for 2 h. To this was added 134 μL H_2O, 0.9 μL 1 M Tris-HCl pH 7.5, 3.75 μL 20 mM $CaCl_2$ and 1 μL 10 U/μL DNase I (Invitrogen) and the mixture was incubated for another 20 min at 37°C. The mixture was extracted with phenol/$CHCl_3$, precipitated with NaCl/EtOH, dried and redissolved in 5 μL of H_2O. A 5 μL volume of labeling mastermix (29 uL H_2O, 10 uL PNK-buffer (NEB), 1 uL [^{32}P]γ-ATP (Perkin-Elmer) and 10 uL PNK (NEB)) were added and the mixture was incubated at 37°C for 1 h. The resulting short labeled RNA fragments were resolved on a 20 % denaturing polyacrylamide gel in order to monitor correct extension of ai5γ-1.

Reaction with fluorescein isothiocyanate

Intron RNAs containing 3′-terminal uridine or 2′-aminouridine residue (20 pmols) were 5′-^{32}P labeled and then resuspended in 8 μl of water. Then 12 μl of 0.5 M $NaHCO_3$ buffer (pH9.2) and 1 mg of fluorescein isothiocyanate (Sigma) dissolved in 20 μl dimethyl formamide were added. Reaction mixtures were incubated overnight at 4 °C, RNAs were ethanol precipitated, purified from unreacted FITC on a MEGAclear column (Ambion) and analyzed on a 5% denaturing polyacrylamide gel. In order to detect ^{32}P label, bands were visualized on a Storm 820 Phosphorimager (Molecular Dynamics), and in order to detect fluorescein label, bands were visualized using an FLA-5100 scanner (Fujifilm).

In order to further confirm the covalent attachment of FITC to the 2′-amino group, extended intron RNA containing 3′-terminal 2′-aminouridine was cleaved with DNAzyme 3 (see above) before and after reaction with FITC. The DNAzyme cleavage reaction was carried out for 2 hours under the same conditions as described above for DNAzymes 1 and 2. Resulting fragments were 5′-end labeled and analyzed on a 20% polyacrylamide gel.

Reverse-splicing assays and timecourses

Single turnover experiments were carried out using 100 nM intron and trace amounts (2 nM) of 3′-end labeled substrate at 42 °C in 40 mM MES-KOH (pH 4.8 – 6.4) or MOPS-KOH (pH 6.3 – 7.8), 100 mM $MgCl_2$ and 500 mM KCl11,44. Intron and substrate were separately denatured in 80 mM MOPS-KOH or MES-KOH for 1 minute at 95 °C and cooled for 1 minute to 42°C. Salts were added, allowing the intron and substrate to fold independently for 10 minutes before they were combined. Aliquots were taken after increasing reaction times, and these were immediately mixed with 4 volumes of quench buffer (75% formamide

and 50 mM EDTA) and stored on ice until products were separated on stacked polyacrylamide gels (5% and 20 %). The gels were dried and exposed to phosphorimager plates for imaging on a Storm Imager (Molecular Dynamics).

Calculation and analysis of reaction rate constants

For each experiment, a total of 15 lanes corresponding to different timepoints was analyzed. Bands corresponding to substrate, reverse-splicing product and SER product were quantified using ImageQuant software (Molecular Dynamics) and their volumes (within each lane) were normalized to 1. In order to extract the rate constants for reverse splicing, the resulting datasets were analyzed by a least-squares fitting procedure based on the model shown in Figure 1c using the kinetic simulation software package Dynafit (BioKin, Ltd.)27. The pH dependence of reverse-splicing by the $2'NH_2$-modified intron was analyzed by plotting the reverse-splicing rate constants against the respective pH values (Supplementary Figure 2) and fitting them to equation 1 using Origin software (OriginLab).

Supplementary Material

Refer to Web version on PubMed Central for supplementary material.

Acknowledgments

We wish to thank C.M. Joyce for providing the E710A mutant protein. This work was supported by generous funding from the NIH (GM50313) and from the Howard Hughes Medical Institute. A.M.P. is an investigator of the Howard Hughes Medical Institute.

References

1. Pyle, AM.; Lambowitz, AM. Group II introns: Ribozymes that splice RNA and invade DNA. In: Gesteland, RF.; Cech, TR.; Atkins, JF., editors. The RNA world. Cold Spring Harbor Laboratory Press; Cold Spring Harbor, New York: 2006. p. 469-505.
2. Vallès Y, Halanych KM, Boore JL. Group II Introns Break New Boundaries: Presence in a Bilaterian's Genome. PLoS ONE. 2008; 3:e1488. [PubMed: 18213396]
3. Pyle, AM. Group II Introns: Catalysts for Splicing, Genomic Change and Evolution. In: Lilley, DMJ.; Eckstein, F., editors. Ribozymes and RNA Catalysis. RCS Publishing; Cambridge, U.K: 2008. p. 201-228.
4. de Lencastre A, Hamill S, Pyle AM. A single active-site region for a group II intron. Nat Struct Mol Biol. 2005; 12:626–7. [PubMed: 15980867]
5. Toor N, Keating KS, Taylor SD, Pyle AM. Crystal structure of a self-spliced group II intron. Science. 2008; 320:77–82. [PubMed: 18388288]
6. Toor N, Rajashankar K, Keating KS, Pyle AM. Structural basis for exon recognition by a group II intron. Nat Struct Mol Biol. 2008; 15:1221–2. [PubMed: 18953333]
7. Dai L, et al. A three-dimensional model of a group II intron RNA and its interaction with the intron-encoded reverse transcriptase. Mol Cell. 2008; 30:472–85. [PubMed: 18424209]
8. Daniels DL, Michels WJ Jr, Pyle AM. Two competing pathways for self-splicing by group II introns: a quantitative analysis of in vitro reaction rates and products. J Mol Biol. 1996; 256:31–49. [PubMed: 8609612]
9. Chu VT, Liu Q, Podar M, Perlman PS, Pyle AM. More than one way to splice an RNA: branching without a bulge and splicing without branching in group II introns. RNA. 1998; 4:1186–202. [PubMed: 9769094]
10. Podar M, Perlman PS, Padgett RA. The two steps of group II intron self-splicing are mechanistically distinguishable. RNA. 1998; 4:890–900. [PubMed: 9701281]

11. Roitzsch M, Pyle AM. The linear form of a group II intron catalyzes efficient autocatalytic reverse splicing, establishing a potential for mobility. RNA. 2009; 15:473–82. [PubMed: 19168748]
12. Aizawa Y, Xiang Q, Lambowitz AM, Pyle AM. The pathway for DNA recognition and RNA integration by a group II intron retrotransposon. Mol Cell. 2003; 11:795–805. [PubMed: 12667460]
13. Roitzsch, M. Wiley Encyclopedia of Chemical Biology. John Wiley & Sons; Hoboken: 2008. Group II Introns.
14. Padgett RA, Podar M, Boulanger SC, Perlman PS. The stereochemical course of group II intron self-splicing. Science. 1994; 266:1685–8. [PubMed: 7527587]
15. Gordon PM, Piccirilli JA. Metal ion coordination by the AGC triad in domain 5 contributes to group II intron catalysis. Nat Struct Biol. 2001; 8:893–8. [PubMed: 11573097]
16. Podar M, Perlman PS, Padgett RA. Stereochemical selectivity of group II intron splicing, reverse splicing, and hydrolysis reactions. Mol Cell Biol. 1995; 15:4466–78. [PubMed: 7542746]
17. Sontheimer EJ, Gordon PM, Piccirilli JA. Metal ion catalysis during group II intron self-splicing: parallels with the spliceosome. Genes Dev. 1999; 13:1729–41. [PubMed: 10398685]
18. Gordon PM, Fong R, Piccirilli JA. A Second Divalent Metal Ion in the Group II Intron Reaction Center. Chem Biol. 2007; 14:607–12. [PubMed: 17584608]
19. Steitz TA, Steitz JA. A general two-metal-ion mechanism for catalytic RNA. Proc Natl Acad Sci USA. 1993; 90:6498–502. [PubMed: 8341661]
20. Griffin EA Jr, Qin Z, Michels WJ Jr, Pyle AM. Group II intron ribozymes that cleave DNA and RNA linkages with similar efficiency, and lack contacts with substrate 2′-hydroxyl groups. Chem Biol. 1995; 2:761–70. [PubMed: 9383483]
21. Gordon PM, et al. New strategies for exploring RNA's 2′-OH expose the importance of solvent during group II intron catalysis. Chem Biol. 2004; 11:237–46. [PubMed: 15123285]
22. Huang Z, Szostak JW. A simple method for 3′-labeling of RNA. Nuc Acids Res. 1996; 24:4360–1.
23. Milligan JF, Groebe DR, Witherell GW, Uhlenbeck OC. Oligoribonucleotide synthesis using T7 RNA polymerase and synthetic DNA templates. Nucleic Acids Res. 1987; 15:8783–98. [PubMed: 3684574]
24. Kao C, Rüdisser S, Zheng M. A simple and efficient method to transcribe RNAs with reduced 3′ heterogeneity. Methods. 2001; 23:201–5. [PubMed: 11243833]
25. Astatke M, Ng K, Grindley ND, Joyce CM. A single side chain prevents Escherichia coli DNA polymerase I (Klenow fragment) from incorporating ribonucleotides. Proc Natl Acad Sci USA. 1998; 95:3402–7. [PubMed: 9520378]
26. Pyle AM, Chu VT, Jankowsky E, Boudvillain M. Using DNAzymes to cut, process, and map RNA molecules for structural studies or modification. Methods Enzymol. 2000; 317:140–6. [PubMed: 10829278]
27. Kuzmic P. Program DYNAFIT for the analysis of enzyme kinetic data: Application to HIV proteinase. Anal Biochem. 1996; 237:260–273. [PubMed: 8660575]
28. Dunitz JD, Taylor R. Organic Fluorine Hardly Ever Accepts Hydrogen Bonds. Chem Eur J. 1997; 3:89–98.
29. Aurup H, Tuschl T, Benseler F, Ludwig J, Eckstein F. Oligonucleotide duplexes containing 2′-amino-2′-deoxycytidines: thermal stability and chemical reactivity. Nuc Acids Res. 1994; 22:20–4.
30. Shan SO, Herschlag D. Probing the Role of Metal Ions in RNA Catalysis: Kinetic and Thermodynamic Characterization of a Metal Ion Interaction with the 2′-Moiety of the Guanosine Nucleophile in the Tetrahymena Group I Ribozyme. Biochemistry. 1999; 38:10958–10975. [PubMed: 10460151]
31. Roitzsch M, Anorbe MG, Sanz Miguel PJ, Müller B, Lippert B. The role of intramolecular hydrogen bonding on nucleobase acidification following metal coordination: possible implications of an "indirect" role of metals in acid-base catalysis of nucleic acids. J Biol Inorg Chem. 2005; 10:800–12. [PubMed: 16231130]
32. Serjeant, EP.; Dempsey, B., editors. IUPAC Chem. Data Ser. No. 23. Pergamon Press; Oxford, UK: 1979. Ionization Constants of Organic Acids in Solution.

33. Sigel RK, Vaidya A, Pyle AM. Metal ion binding sites in a group II intron core. Nat Struct Biol. 2000; 7:1111–6. [PubMed: 11101891]
34. Yoshida A, Shan S, Herschlag D, Piccirilli JA. The role of the cleavage site 2′-hydroxyl in the Tetrahymena group I ribozyme reaction. Chem Biol. 2000; 7:85–96. [PubMed: 10662698]
35. Oyelere AK, Kardon JR, Strobel SA. pK(a) perturbation in genomic Hepatitis Delta Virus ribozyme catalysis evidenced by nucleotide analogue interference mapping. Biochemistry. 2002; 41:3667–75. [PubMed: 11888283]
36. Das SR, Piccirilli JA. General acid catalysis by the hepatitis delta virus ribozyme. Nat Chem Biol. 2005; 1:45–52. [PubMed: 16407993]
37. Gordon PM, Sontheimer EJ, Piccirilli JA. Kinetic characterization of the second step of group II intron splicing: role of metal ions and the cleavage site 2′-OH in catalysis. Biochemistry. 2000; 39:12939–52. [PubMed: 11041859]
38. Weinger JS, Parnell KM, Dorner S, Green R, Strobel SA. Substrate-assisted catalysis of peptide bond formation by the ribosome. Nat Struct Mol Biol. 2004; 11:1101–6. [PubMed: 15475967]
39. Lang K, Erlacher M, Wilson DN, Micura R, Polacek N. The role of 23S ribosomal RNA residue A2451 in peptide bond synthesis revealed by atomic mutagenesis. Chem Biol. 2008; 15:485–92. [PubMed: 18439847]
40. Gordon PM, Sontheimer EJ, Piccirilli JA. Metal ion catalysis during the exon-ligation step of nuclear pre-mRNA splicing: extending the parallels between the spliceosome and group II introns. RNA. 2000; 6:199–205. [PubMed: 10688359]
41. Wincott F, et al. Synthesis, deprotection, analysis and purification of RNA and ribozymes. Nuc Acids Res. 1995; 23:2677–84.
42. England TE, Uhlenbeck OC. 3′-terminal labelling of RNA with T4 RNA ligase. Nature. 1978; 275:560–1. [PubMed: 692735]
43. Polesky AH, Dahlberg ME, Benkovic SJ, Grindley ND, Joyce CM. Side chains involved in catalysis of the polymerase reaction of DNA polymerase I from Escherichia coli. J Biol Chem. 1992; 267:8417–28. [PubMed: 1569092]
44. Fedorova O, Su LJ, Pyle AM. Group II introns: highly specific endonucleases with modular structures and diverse catalytic functions. Methods. 2002; 28:323–35. [PubMed: 12431436]

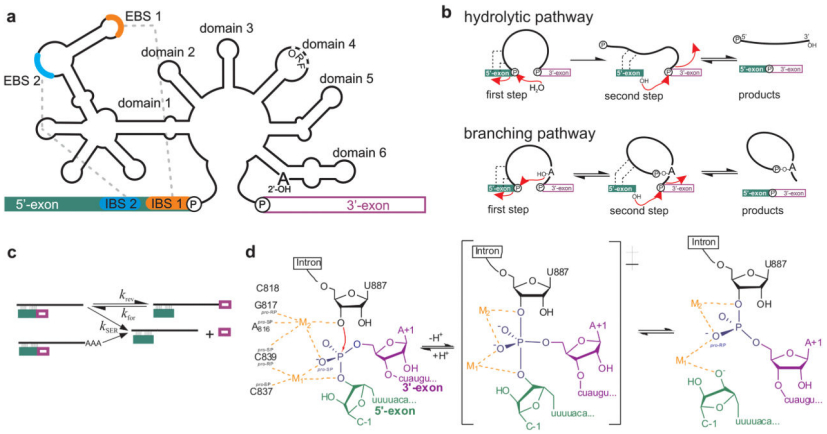

Figure 1.

Structure and splicing pathways of group II introns. **a** Consensus secondary structure of group II introns. The intron is shown as a black line and the 5′-and 3′-exon as a filled green or open purple bar, respectively. The scissile phosphates at the 5′-and 3′-splice sites are depicted as encircled “P”s. Exon binding sites EBS 1 and EBS 2 in domain 1, the corresponding intron binding sites IBS 1 and IBS 2 on the 5′-exon, the open reading frame (ORF) in domain 4 and the branching point adenosine in domain 6 are indicated. **b** Schematic of the splicing process by hydrolysis (top) and branching (bottom). **c** Kinetic framework of reverse-splicing and SER by linear intron. Intron molecules with untemplated nucleotides at the 3′-end are indicated as a straight line with a stretch of “A”s. **d** Mechanistic model for reversal of the second splicing step. Nucleotide sequences and numbering are corresponding to the original ai5γ intron from *S. cerevisiae*. Sections of the intron are shown in the same colors as before, the scissile phosphate is displayed in blue, metal ions and coordinative bonds in orange.

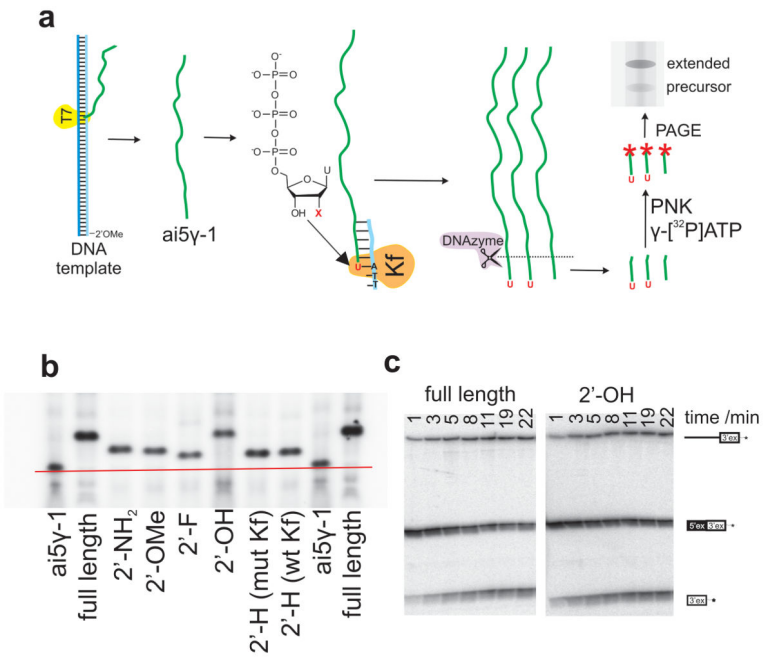

Figure 2.

Synthesis and verification of intron RNAs with substitutions of the 2′-OH group at the 3′-terminal nucleotide. **a** Schematic of the extension and verification method. DNA strands are shown as blue, RNA as green lines. The enzymes used were T7 RNA polymerase (T7, yellow), the E710A mutant of the Klenow fragment (Kf, orange) and DNAzyme (purple). The dotted line indicates the DNAzyme cleavage site. The 2′-substituent introduced with the terminal nucleotide is shown as a bold red X. **b** Gel showing terminal fractions of the modified introns. A negative control using transcripts that lack the terminal nucleotide (ai5γ-1) and a positive control using a full length transcript are shown in the left and right two lanes; the bands of the ai5γ-1 precursor are connected by a thin red line for better readability. Substituents introduced into the respective RNAs are indicated; 2′-deoxythymidine (2′-H) was introduced according to the same protocol as the other substituents (mut. Kf) and, for comparison, with commercially available wild-type Klenow fragment (wt Kf). **c** Control showing reverse-splicing catalyzed by the transcribed full-length wild-type intron (left) and by wild-type intron generated through extension of ai5γ-1 with rUTP(right) at pH 6.0. Assignments of substrate and product bands as well as reaction times are indicated.

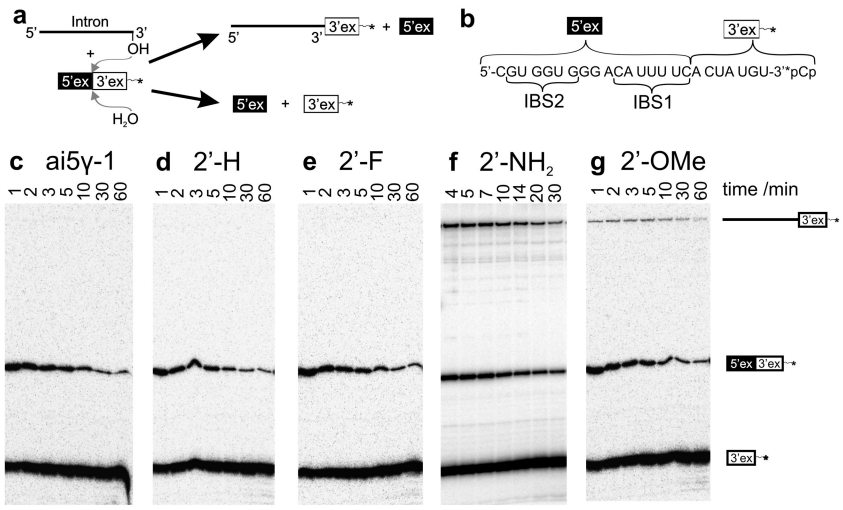

Figure 3.

Reverse-splicing assay. **a** Schematic of the reverse-splicing reaction. Intron is depicted as a black line, 5′- and 3′-exons as filled and open boxes, respectively. The radiolabel at the 3′-terminus of the substrate is indicated by an asterisk. **b** Sequence of the RNA substrate. 5′- and 3′-exon sections as well as intron binding sites IBS1 and IBS2 and the radiolabel at the 3′-end are indicated. **c**-**g** Time courses performed with the intron analogs at pH 7.8. The substitution applied to the terminal nucleotide of each RNA is indicated. Assignments of precursor and product bands as well as reaction times are shown on the right side.

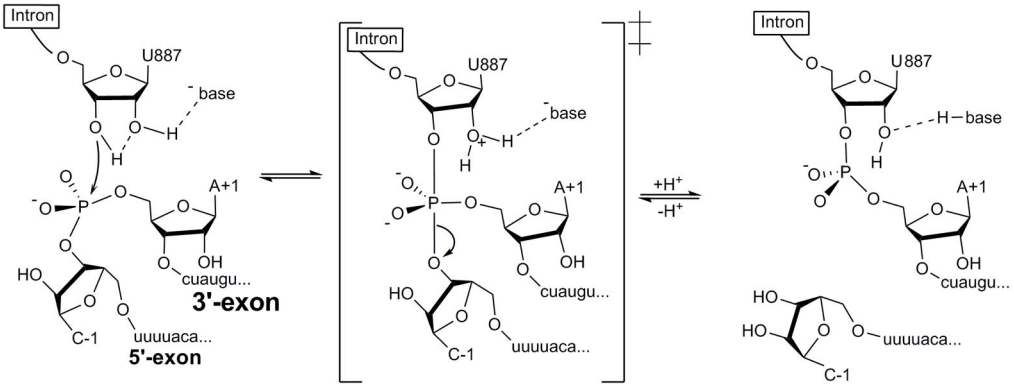

Figure 4.

Suggested proton shuttle mechanism. Sequences and numbering refer to the original ai5γ intron. Hydrogen bonds are shown as dotted lines. Metal ions have been omitted for clarity.

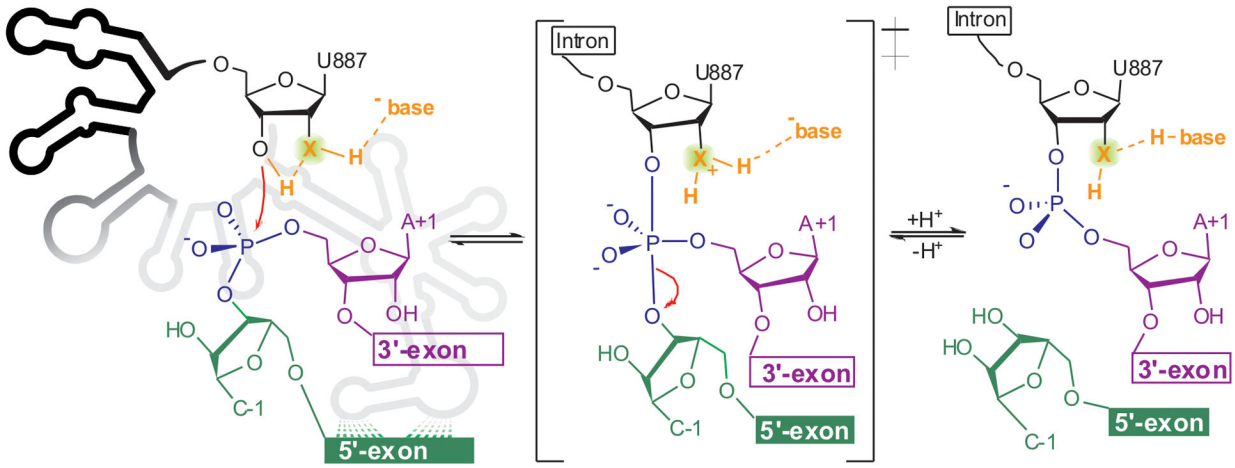

Figure 5.